



2016

## Resonant Collisions of Potassium Atoms

Philip Michael Adamson  
*Colby College*

Follow this and additional works at: <https://digitalcommons.colby.edu/honortheses>

 Part of the [Atomic, Molecular and Optical Physics Commons](#), and the [Quantum Physics Commons](#)

Colby College theses are protected by copyright. They may be viewed or downloaded from this site for the purposes of research and scholarship. Reproduction or distribution for commercial purposes is prohibited without written permission of the author.

---

### Recommended Citation

Adamson, Philip Michael, "Resonant Collisions of Potassium Atoms" (2016). *Honors Theses*. Paper 831.

<https://digitalcommons.colby.edu/honortheses/831>

# **Resonant Collisions of Potassium Atoms**

Philip M. Adamson

A thesis presented to the faculty of the  
Department of Physics and Astronomy at  
Colby College

Department of Physics and Astronomy  
Colby College  
Waterville, ME  
May, 2016

**ABSTRACT.** This thesis discusses an approach to excite potassium atoms to very highly excited states (Rydberg states), and then tune their energy levels to induce resonant collisions between atoms. Potassium gas is super-cooled to 1 mK and confined to a small volume in a magneto-optical trap. A 405 nm laser diode, electronically locked to a potassium vapor cell via Doppler free spectroscopy, excites these atoms from the  $4s_{1/2}$  state (ground state) to the  $5p_{3/2}$  state. A 978 nm laser then excites the  $5p_{3/2}$  to  $nd_{3/2}$  or  $nd_{5/2}$  transition, creating Rydberg atoms. Since there is no ground state reference for this transition, an alternative method must be used to lock the laser's frequency. A scanning transfer cavity lock transfers the stability of a 632 nm HeNe reference laser to the unstable 978 nm laser diode by passing both lasers through a Fabry-Pérot interferometer. Once Rydberg atoms have been created, their energy levels are tuned with an external electric field so that collisions between atoms cause resonant atomic transitions to different Rydberg states. The Rydberg atoms are ionized with a second, stronger electric field, and detected by microchannel plate detectors. Rydberg atoms with different principal quantum numbers ionize at different electric field strengths, so a successful collision signal has multiple peaks from the microchannel plates.

## Acknowledgments

I would like to thank Professor Charles Conover for his immense help and support throughout my research experience dating back to last summer, and throughout the thesis process. I am grateful for his advice and guidance, and inspired by his passion for this subject.

I would like to thank the Colby College Department of Physics and Astronomy. I am lucky to have had such great professors in my time here, who have dedicated countless hours to answering my questions, guiding me through difficult topics, and assisting me in my job search. My passion for physics, problem solving, and asking questions could not have been achieved without you. I would also like to thank my fellow physics classmates for long nights in Mudd, often made better by pizza.

Finally, I would like to thank my parents Peter and Susanne, and my siblings Eric, Jacob and Julia, for their unending support and encouragement.

# Contents

<b>1</b>	<b>Introduction</b>	<b>4</b>
1.1	Rydberg Atoms . . . . .	4
1.2	Motivation . . . . .	5
<b>2</b>	<b>Experiment</b>	<b>7</b>
2.1	Experimental Overview . . . . .	7
2.2	External Cavity Diode Lasers . . . . .	9
2.3	Magneto-Optical Trap . . . . .	10
2.4	Rydberg Excitement: Stage I . . . . .	13
2.4.1	Setup . . . . .	13
2.4.2	Frequency Stabilization: Doppler Free Spectroscopy . . . . .	14
2.5	Rydberg Excitement: Stage II . . . . .	17
2.5.1	Setup . . . . .	17
2.5.2	Acousto-Optic Modulator . . . . .	19
2.5.3	Frequency Stabilization: Scanning Transfer Cavity Lock . . . . .	20
2.6	Rydberg State Detection . . . . .	24
2.6.1	Field Ionization . . . . .	24
2.6.2	Microchannel Plate Detector . . . . .	26
2.7	Resonant Collisions . . . . .	27
<b>3</b>	<b>Results and Discussion</b>	<b>32</b>
3.1	Scanning Transfer Cavity Lock Frequency Stabilization . . . . .	32
3.2	Rydberg State Detection . . . . .	34
3.3	Resonant Collisions . . . . .	36
3.4	Stark Shifts . . . . .	36
<b>4</b>	<b>Conclusion</b>	<b>40</b>

# 1 Introduction

## 1.1 Rydberg Atoms

A Rydberg atom is any atom that contains one or more electrons with a high principal quantum number. That is, one or more electrons that have been excited to very high energy states, with large radii, but still bound by the nucleus. The classical picture of a neutral Rydberg atom is one electron located on a vastly extended orbit far from the nucleus. The inner electrons remain close to the nucleus, so the outer electron “sees” the nucleus as a small positive charge consisting of the nucleus and all but one electron. Therefore, a neutral Rydberg atom is a good approximation of a hydrogen-like system, which greatly simplifies the quantum mechanical description of the atom. The energy levels, for instance, are very close to those for a hydrogen atom,

$$E = -\frac{Ry}{(n - \delta_l)^2} \quad (1)$$

where  $\delta$  is the quantum defect and  $Ry$  is the Rydberg constant [1]. The quantum defect is a function of angular momentum  $l$ , and is due to low angular momentum electrons penetrating the inner cloud of electrons during certain locations of its orbit, so it “knows” the Rydberg atom is not truly hydrogen-like. This quantum defect is approximately zero for  $l > 3$ . Like hydrogen, the radius of the orbit increases as the square of the principal quantum number,

$$r = a_0 n^2 \quad (2)$$

where  $a_0$  is the Bohr radius [1]. For large principal quantum numbers, atomic radii become enormous. A potassium atom has a radius of approximately one Angstrom, while a potassium Rydberg atom can have a radius of thousands of Angstroms.

The hydrogen-like nature of Rydberg atoms leads to some interesting properties. Due to the large radial orbit of the valence electron, Rydberg atoms have a very large dipole moment from the separation of positive and negative charge. While ground state atoms are relatively unaffected by electric fields, the large dipole moment of Rydberg atoms gives them a large response to external electric fields. For instance, valence electrons in Rydberg atoms can be ionized with an external electric field [1]. Their energy levels can be shifted with electric fields, known as Stark shifting.

The large dipole moments also lead to very strong interactions between Rydberg atoms. They can interact and “feel” each other, quantum mechanically, over long ranges. This could be used to entangle states to create gates for quantum computing. Another useful property of Rydberg atoms is their long lifetimes compared to “normal” excited states, on the order of tens to even hundreds of microseconds [1]. Lifetimes of Rydberg atoms are proportional to  $n^3$ . This makes it possible to study gases of Rydberg atoms that are stable and won’t spontaneously decay faster than they can be studied. Finally, Rydberg atomic energy levels are nicely spaced so it is easy to selectively excite states.

## 1.2 Motivation

Their long lifetimes, selectively excitable and detectable energy states, and sensitivity to external electric fields make Rydberg atoms useful for studying some basic problems in quantum dynamics. For instance, consider the two level system, the simplest nontrivial problem in quantum mechanics. In a two-level system, atoms can populate two energy levels, and we want to know the population of each state as a function of time after an electromagnetic pulse is applied to the system. While the problem seems simple enough, there are only a few pulses for which there exist analytical solutions. There remains a lot to be learned by actually doing experiments in the lab.

Another ‘simple’ quantum mechanical process that is quite interesting to study, and the one considered in this thesis, are resonant collisions. Resonant collisions in an ultracold gas are not physical collisions, but rather resonant dipole-dipole energy exchanges between two atoms. These energy exchanges occur when one atom loses as much internal energy as another gains [2]. Since the energy levels in Rydberg atoms are easily shifted via the Stark effect, well chosen atomic states can be tuned into resonance using only moderate electric fields. In practice, the energy transfers should be dominated by dipole-dipole interactions rather than thermal effects. It is desirable then to study ultra cold Rydberg atoms in a magneto-optical trap, or “frozen gases” with temperatures of hundreds of  $\mu K$  (and small atomic velocities). Resonant dipole-dipole energy transfers have been observed in frozen Rydberg gases primarily in rubidium [2,4,5], but also in cesium [6,7]. The experiment described in this thesis is the first attempt to induce these resonant energy transfers in ultra cold potassium Rydberg atoms.

Perhaps the most interesting application of Rydberg atoms is their potential for use in con-

structing a fast quantum gate, and in turn, quantum computers. The long-range dipole forces exhibited by Rydberg atoms make them “particularly well suited for quantum information processing” [2]. The idea to use Rydberg interactions for neutral atom quantum gates was first proposed in 2000 in the paper *Fast Quantum Gates for Neutral Atoms* [8]. Since then, the idea has been expanded to mesoscopic ensembles of many Rydberg atoms [9]. In these systems, quantum processing is achieved via the “dipole blockade.” A laser resonant with an atomic transition frequency excites Rydberg atoms when they are far apart. As the internuclear distance decreases, the dipole-dipole interactions shift the Rydberg pair out of resonance with the laser [2]. Atoms around each Rydberg atom are “blocked” from becoming excited, resulting in optically addressable domains [2]. The Rydberg blockade makes it possible to excite a single atom, which would typically require very high optical resolution [2]. The dipole blockade, combined with the long coherence time of Rydberg atoms, allow for the creation of superpositions of spin states, and the ability to perform quantum gate operations between distant qubits [9].

The prospects of Rydberg atoms for implementing quantum information processing was explored in detail by [2]. They considered three possibilities to create the strong inter-particle forces required for fast quantum gates: van der Waals interactions, interactions of permanent dipoles, and resonant resonant energy transfer collisions [2]. They found that resonant energy transfer collisions, or Förster resonances, “seems to be the most promising approach for the implementation of quantum information processing in Rydberg atoms” [2]. The resonant energy collisions are of interest because a change in electric field turns two Rydberg atoms from on resonance to off resonance, changing the strength of their interaction by more than an order of magnitude [2]. This allows for fine control of the interaction process. Dipole-dipole resonant collisions in Rydberg atoms have been an exciting topic of research [2, 3]. The resonant collisions explored in this paper offer both a way to learn more about the nature of a simple quantum mechanical system, and could offer insights into one of the most exciting technological possibilities quantum mechanics has to offer, the quantum computer.

## 2 Experiment

### 2.1 Experimental Overview

The goal of the experiment described in this thesis is to induce resonant collisions in ultra-cold potassium Rydberg atoms. The approach is to excite Rydberg states in potassium atoms, tune their energy levels with an external electric field, and then detect resonant collisions by ionizing and detecting electrons. An overview of the experimental setup is given in Figure 1. Potassium atoms are heated to a vapor and contained in an Ultra-High Vacuum with a pressure of  $2 \times 10^{-10}$  Torr. The atoms are trapped in a magneto-optical trap (MOT) to create a dense, slowly moving cloud of gas in the center of the chamber. The magneto-optical trap consists of a magnetic field, and a Doppler cooling laser (770 nm) which excites the  $4s_{1/2}$  to  $4p_{3/2}$  transition. All lasers in this experiment are external cavity diode lasers. Once the atoms are trapped in the MOT, Rydberg atoms are excited in two steps. First, a 405 nm laser shines through the potassium atom vapor cloud to excite atoms from the ground state ( $4s_{1/2}$ ) to the  $5p_{3/2}$  state. A 978 nm laser then excites the atoms in the  $5p_{3/2}$  state to the  $40d_{3/2}$  or  $40d_{5/2}$  state. Atoms in the  $40d$  state are considered Rydberg atoms. An energy level diagram of this excitation strategy is given in Figure 2. Once Rydberg atoms have been created, voltages applied to four conducting rods create an electric field to either Stark shift energy levels, or ionize the electrons from the Rydberg atoms. A microchannel plate detector detects electrons from these Rydberg atoms. The detector produces a current proportional to the number of electrons that hit it, and serves as a way to collect data about the Rydberg atoms.

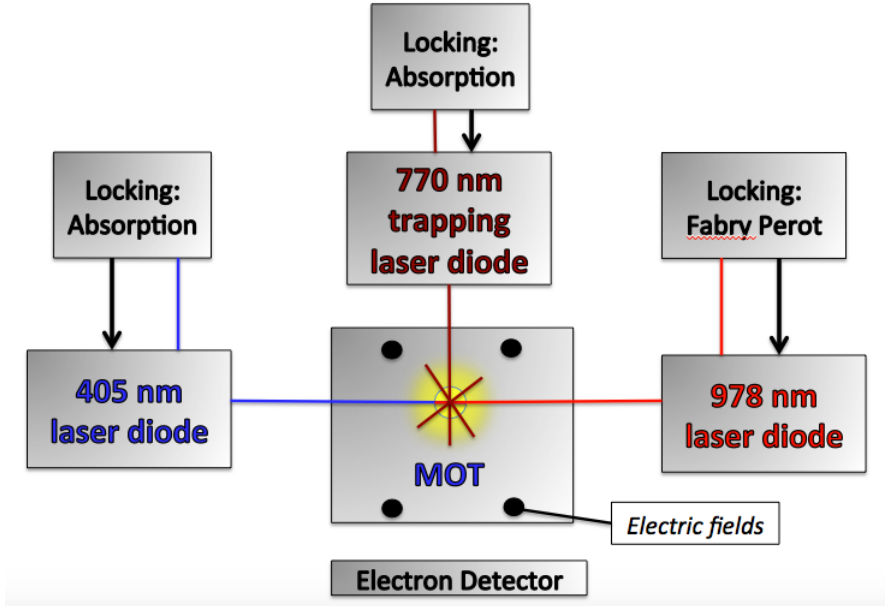


Figure 1: Experimental Overview. Potassium atoms are super-cooled in a magneto-optical trap with a 770 nm laser diode and a magnetic field. The MOT contains 4 conducting rods used to produce electric fields. Two diode lasers, with wavelengths of 405 nm and 978 nm, excite Rydberg states in the atoms. Each laser contains a mechanism of externally locking its frequency. An electron detector is used to detect electrons from Rydberg atoms.

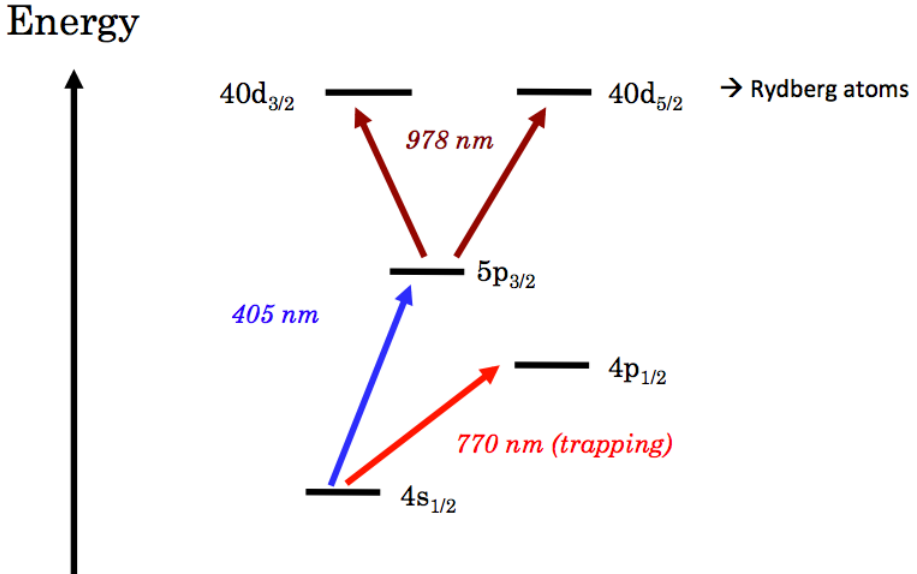


Figure 2: Energy level diagram of the excitation scheme to produce Rydberg atoms.

## 2.2 External Cavity Diode Lasers

This experiment uses three external cavity diode lasers (ECDLs) that produce coherent light with wavelengths of 405 nm, 770 nm, and 978 nm. Diode lasers are widespread in atomic physics experiments due to their high reliability and low price [10]. Like a light emitting diode (LED), a diode laser contains a direct bandgap semiconductor. When an adequate voltage is applied, electrons from the n-doped region in the conduction band and holes from the p-doped region in the valence band combine in the active region [11]. The loss of energy in the recombination of an electron and a hole emits a photon. In an LED, electrons and holes recombine via spontaneous recombination, and emit photons at random times and in random directions [11]. In a diode laser, a photon stimulates the recombination of an electron and a hole while also generating a new photon with the same frequency, direction, and phase. The result is a net gain in photons, which results in the positive optical gain required for a laser. This is known as stimulated recombination, and results in coherent photon emission [11]. Altering the current or temperature of the diode laser can make small adjustments to its frequency [12].

When scanning the laser frequency with only current adjustments, there may be gaps in frequencies and the laser frequency may jump. An external cavity coupled with the diode laser can alleviate this problem, while also decreasing the bandwidth of the emitted light [12]. The external cavity contains a diffraction grating, and its 0th order beam is emitted. Changing the angle of the diffraction grating and length of the cavity can tune the frequency of the laser up to tens of nanometers [21]. Applying a voltage to a piezoelectric transducer attached to the diffraction grating makes small adjustments to the angle of the grating and the spacing between the grating and the diode, and thus the frequency of light emitted by the laser diode. A schematic of the first external cavity diode laser to use this setup is given in Figure 3. An image of one of the external cavity diode lasers used in our lab is given in Figure 4. The frequency of these diode lasers will drift over time due to atmospheric changes in temperature, pressure, and humidity. Even very small drifts, on the order of MHz over hours, are enough to tune the laser out of resonance with an atomic transition. The frequency of the laser diodes must be actively stabilized by placing an electronic signal in feedback with the voltage applied to the piezoelectric transducer.

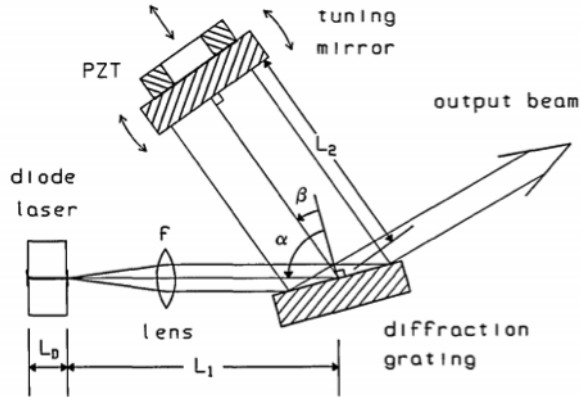


Figure 3: Schematic of the first external cavity diode laser. A similar arrangement is used for the external cavity diode lasers in this experiment. A piezo electric transducer (PZT) adjusts the angle of a diffraction grating and length of the cavity to make fine adjustments to the frequency of light emitted by the laser. Figure taken from [12].

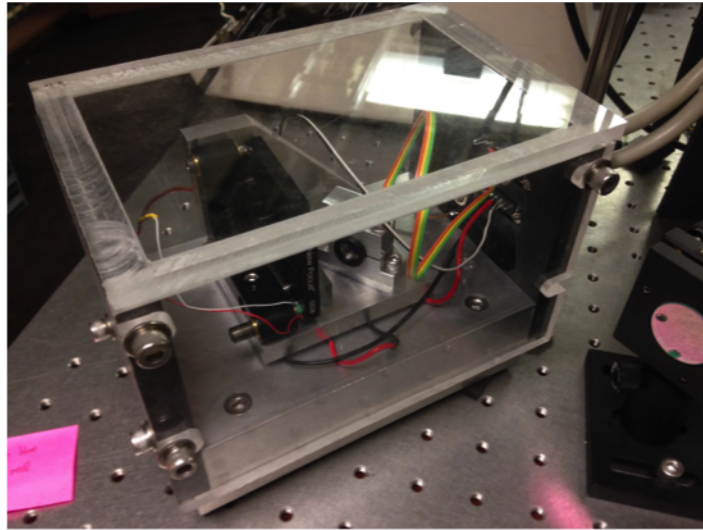


Figure 4: The 770 nm external cavity diode laser. The other two ECDLs used in this experiment look nearly identical, but have some differences in the laser diode used.

### 2.3 Magneto-Optical Trap

A magneto-optical trap uses laser cooling and magnetic fields to create a dense, slowly moving cloud of gas. An Ultra-High Vacuum with  $P_0 \approx 2 \times 10^{-10}$  Torr contains a solid piece of potassium salt. When heated, some of the potassium vaporizes and fills the vacuum chamber with a low concentration of room-temperature potassium gas, raising the pressure to  $P \approx 5 \times 10^{-9}$  Torr. The

goal is to create a super-cooled gas cloud that is immobilized in the center of the vacuum chamber. Two components are necessary to achieve this goal: laser cooling and an external magnetic field. See Figure 5 for a visual representation of this process.

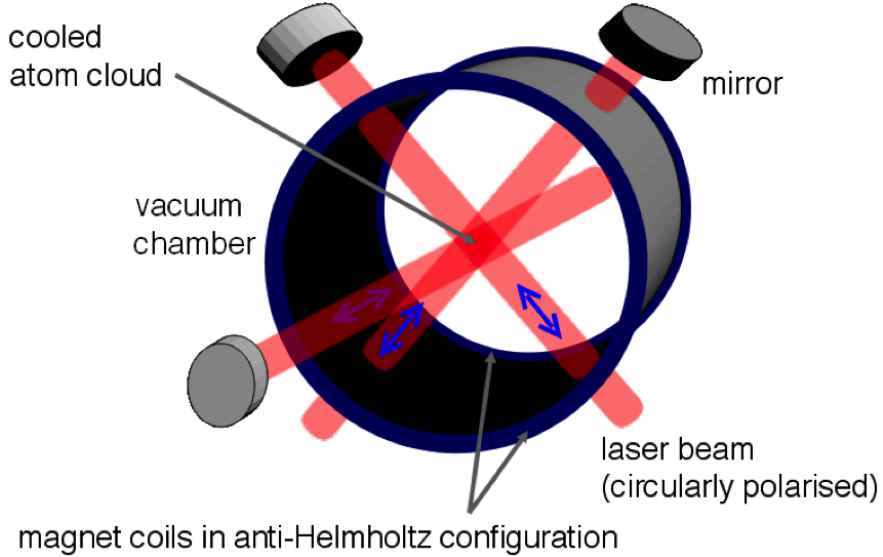


Figure 5: A magneto-optical trap. A vacuum chamber houses some potassium vapor. Six red-detuned laser beams traveling in each direction along the three Cartesian axes laser-cool the atoms. Magnetic coils in an anti-Helmholtz configuration produce a magnetic quadrupole field with its minimum in the center of the vacuum chamber to further cool the atoms via the Zeeman effect. Image taken from [https://commons.wikimedia.org/wiki/File:MOT\\_setup.png](https://commons.wikimedia.org/wiki/File:MOT_setup.png).

The first component in a MOT is Doppler cooling, which aims to cool the gas to very low temperatures. At room temperature, the gas consists of potassium atoms with random motion and an average speed of 440 m/s. In order to slow down the atoms, there must be a transfer of momentum in the opposite direction of the atom's momentum. Photons have a momentum  $p = \frac{h}{\lambda}$  where  $h$  is Planck's constant and  $\lambda$  is the wavelength of the photon. While this momentum is very small compared to the momentum of a potassium atom, a large number of photons colliding with the atoms in the correct orientation will slow the atoms to a crawl ( $\approx 10$  cm/s). Since electron energy levels are quantized, a potassium atom will only collide with (or absorb the momentum of) a photon if the energy of that photon matches the energy needed to excite an electron to a higher energy state. The energy of a photon is proportional to its frequency,  $E = h\nu$ . Tuning a laser to this resonant frequency will bombard atoms with photons that excite electrons and transfer momentum. Due to the Doppler effect, however, the frequency of photons in the rest frame of the

lab is not the same as the frequency in the rest frame of a rapidly moving electron. By setting the laser frequency slightly lower than resonant frequency (known as red detuning), only atoms moving towards the photon source will perceive an upshifted frequency towards resonance and absorb photons. So atoms moving towards a laser source feel a momentum kick in the opposite direction. Three orthogonal lasers, each reflected back in the same direction, cools the atoms in all directions. For this experiment, a 770 nm laser diode red-detuned from resonance excites the  $4s_{1/2}$  to  $4p_{3/2}$  transition.

While laser cooling can decrease the velocities of atoms in the vacuum chamber, a magnetic field is required to obtain trapping. A magnetic quadrupole field is oriented such that the minimum of the field lies at the center of the chamber, at the intersection of the 3 laser beams. An atom that moves away from the center will feel an increased magnetic field. An external magnetic field will split the energy levels of the atom by energy proportional to the magnetic field strength, an effect called Zeeman splitting. As an atom moves further from the minimum in the field, its atomic resonance is shifted closer to the frequency of the laser, and the atom is more likely to absorb a photon that pushes it back towards the center of the trap. Careful selection of the circular light polarization ensures the atoms will absorb photons that kick them towards the center, rather than photons that push them further away.

The most important parameters of the MOT cloud for this experiment are its temperature and density. The MOT cloud is about 1 mm in diameter and contains on the order of  $10^6$  to  $10^7$  atoms. The average interatomic spacing can be estimated at approximately  $100\text{-}1000 \mu\text{m}$ . The temperature of the cloud is  $\approx 1 \text{ mK}$ , which means the average atomic velocity is 0.8 m/s. Each cycle in the experiment lasts around  $10 \mu\text{s}$ , so an atom will move about  $10 \mu\text{m}$ , only a few percent of the interatomic spacing. On the timescale of a single experiment, the atoms are essentially fixed in space, a frozen gas. This is important in practice because one does not want atoms to leave the trap after they have been excited, but before a measurement can be taken. It is also important for resonant collisions, where the energy transfer should be dominated by dipole-dipole field interactions, and not thermal effects.

## 2.4 Rydberg Excitement: Stage I

### 2.4.1 Setup

A laser exciting the  $4s_{1/2}$  to  $4p_{3/2}$  transition traps potassium atoms in the MOT. Rydberg atoms are then excited in two steps. First, a 405 nm laser excites atoms from the ground state ( $4s_{1/2}$ ) to the  $5p_{3/2}$  state. A 978 nm laser then excites the atoms in the  $5p_{3/2}$  state to the  $40d_{3/2}$  or  $40d_{5/2}$  state. Atoms in the  $40d$  state are considered Rydberg atoms. An energy level diagram of this excitation strategy is given in Figure 2.

The experimental setup for the 405 nm laser is given in Figure 6. The 405 nm light passes through an optical isolator to prevent reflection of the beam from other optics components back into the laser diode cavity. A microscope slide reflects approximately 20% of the light (10% from each face of the slide) into a Thorlabs Fabry Pérot interferometer. The signal from the interferometer can be used to check if the laser lases at a single frequency. See section 2.5.3 for a more complete discussion on Fabry-Pérot interferometers. A second microscope slide reflects 20% of the remaining light to an arrangement of optics used to stabilize the frequency of the laser diode with a potassium vapor cell. The remaining light is sent into a fiber optic cable through a fiber coupler. The cable runs to the magneto optical trap and aims the light through the MOT cloud.

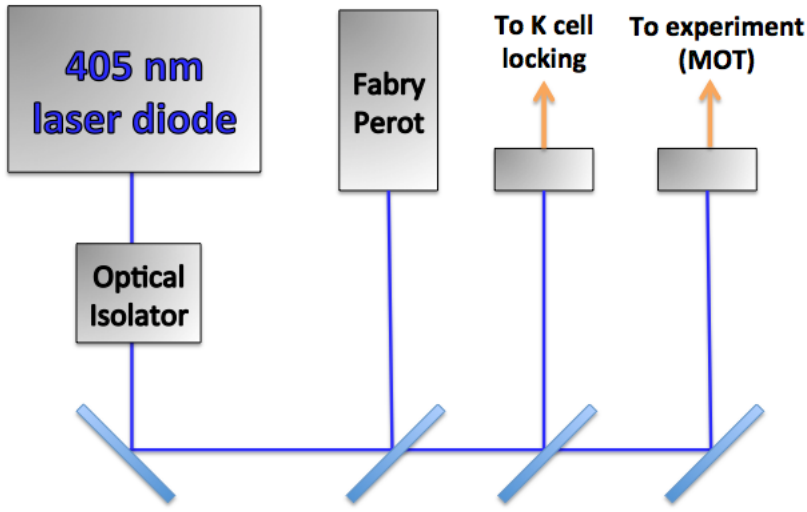


Figure 6: Top-level experimental setup for the first stage of potassium Rydberg atom excitation. Photons from the 405 nm ECDL first pass through an optical isolator to prevent back reflection into the cavity. Light is reflected off of mirrors (leftmost and rightmost blue rectangles) and 20% reflective microscope slides (middle two blue rectangles) to pass light into various components. The Fabry Pérot is used to check if the laser color is a single frequency. Some light is directed to a potassium vapor cell for frequency locking. The rest goes through a fiber optic cable into the MOT.

#### 2.4.2 Frequency Stabilization: Doppler Free Spectroscopy

To optimally excite the  $4s_{1/2}$  to  $5p_{3/2}$  transition, the frequency of the 405nm laser diode should be stable to a part in  $10^8$ , or about 5 MHz. Small changes in room temperature, air pressure, and humidity typically cause the color generated by the laser diode to vary by substantially more than this. Active temperature control and current stabilization of the laser is not sufficient to adequately stabilize the frequency, so a more robust approach is necessary. An electronic signal that exhibits large DC voltage changes for small frequency shifts can be used in a feedback circuit with the laser diode piezo to stabilize the frequency output. The larger the voltage shift per frequency shift, the narrower the frequency range of the locked laser.

The blue laser's frequency dependent electronic signal relies upon Doppler free spectroscopy. Consider a potassium vapor cell filled with potassium gas with transparent panels on either end for light to pass through. Behind the vapor cell is a photodiode that produces a voltage proportional to the intensity of light hitting its detector. For most frequencies, nearly all of the light passes through to the photodiode. For frequencies resonant with an atomic transition, potassium atoms

absorb photons, and less light reaches the photodiode. For stationary atoms, this dip in intensity occurs at a laser frequency equal to the atomic transition frequency. The vapor cell scenario is a bit different, because it contains potassium atoms with a range of velocities moving in random directions. The number of atoms containing a given velocity produces a Gaussian distribution centered on a velocity of zero. Atoms with different velocities (parallel to the photon source) will absorb photons at different frequencies due to Doppler shifting. The number of photons absorbed when plotted versus frequency then also follows a Gaussian distribution. The signal outputted by the photodiode is the baseline light intensity when no absorption occurs minus the intensity of the absorbed photons. As the frequency shifts, the DC output from the photodiode shifts as well.

This Gaussian absorption signal is too broad (not enough voltage change per frequency change) to robustly stabilize the laser frequency. Doppler-free spectroscopy uses a pump-probe scheme to eliminate the problems of Doppler broadening. A laser (the pump beam) is sent through the vapor cell. The beam passes around the vapor cell and back into the cell from the other direction, creating a beam (probe beam) with the same frequency but in the opposite direction. Even though the beams have the same frequency, they will absorb different sets of photons. When the beam is red-detuned from the atomic transition frequency, the pump beam will absorb atoms moving towards the laser, and the probe beam will absorb atoms moving away from the laser at the same velocity (towards the probe beam). When the beam is blue-detuned, the opposite effect will occur. Atoms that have zero velocity (or velocity perpendicular to both beams) will absorb photons from both the pump beam and the probe beam when the laser frequency is resonant with the atomic transition [19].

A photodiode signal from the probe beam when the laser is scanned across a range of frequencies will produce nearly the same Doppler broadened signal as previously discussed. At the frequencies where atoms absorb photons from both beams, the pump beam will excite atoms and depopulate the ground state. This is referred to as the pump beam “burning a hole” in the ground state. These excited atoms cannot absorb another photon from the probe beam, so slightly more light will pass through to the photodiode than would be expected from a normal Doppler broadened signal. There will be slight increases in the absorption signal at frequencies corresponding to atomic transitions (Blue signal in Figure 7) [20].

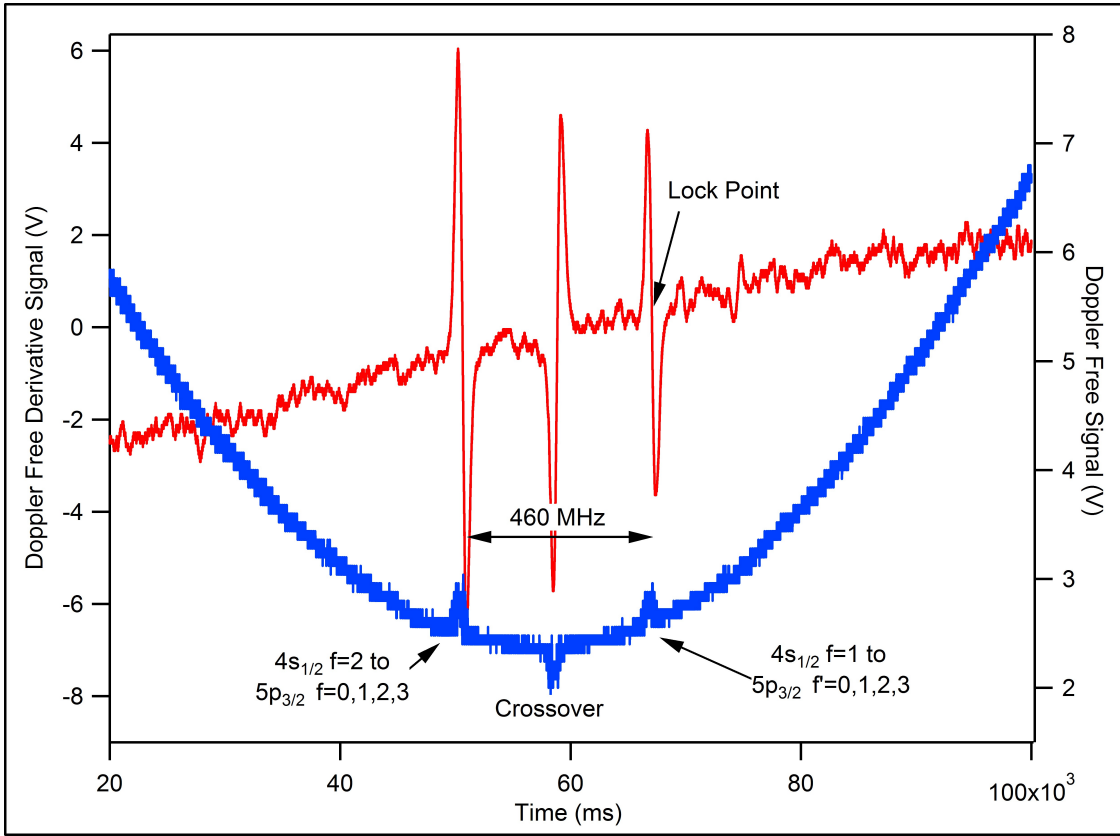


Figure 7: The blue signal (right axis) is the doppler free absorption signal for the 405 nm laser obtained by a frequency scan from scanning the voltage of the PZT on the 405 nm laser diode. The left dip in absorption corresponds to the  $4s_{1/2} f=2$  to  $5p_{1/2} f=0,1,2,3$  transition (Hyperfine structure of the excited state cannot be resolved in this case). The right dip corresponds to the  $4s_{1/2} f=1$  to  $5p_{3/2} f=0, 1, 2, 3$  transition, and the middle dip is the crossover peak. The frequency of the laser is dithered (which is why the blue signal is fuzzy) to produce a derivative signal. The derivative signal is the red signal (left axis). The laser is locked to the frequency where the  $4s_{1/2} f=1$  to  $5p_{3/2}$  transition occurs, a zero point on the derivative signal.

For a system with only two energy levels (a ground state and an excited state), this dip would occur in the center of the Gaussian distribution. However, if there are multiple excited states, the behavior becomes more complicated. Hyperfine splitting of the ground state and the excited state creates multiple dips. In this experiment, only the ground state hyperfine splitting was able to be resolved. The  $4s_{1/2} f=1$  and  $f=2$  to  $5p_{3/2}$  transitions in potassium are within the Doppler broadened frequency range of each other. Their absorption profile is the sum of two Gaussian distributions, creating one bell shaped distribution. There are still dips in absorption at the both the  $4s_{1/2} f=1$  to  $5p_{3/2}$  and  $4s_{1/2} f=2$  to  $5p_{3/2}$  atomic transition frequencies, which appear on either

side of the distribution. At the frequency directly in between these dips, the cross over frequency, the pump and probe beams are resonant with opposite velocity groups (Blue signal in Figure 7). The pump beam excites the  $4s_{1/2}$   $f=1$  atoms to the  $5p_{3/2}$   $f=2$  state. These atoms can decay to either the  $4s_{1/2}$   $f=1$  or  $4s_{1/2}$   $f=2$  state. The probe beam excites the  $4s_{1/2}$   $f=2$  atoms to the  $5p_{3/2}$   $f=1$  state. The pump beam populates the ground state with  $f=2$  atoms, so that the probe beam excites more atoms. The absorption at the crossover frequency is actually larger than the normal Gaussian distribution, as seen in the middle peak in Figure 7. The important feature of this signal for this experiment, however, is the sharper Doppler free features that occur at an atomic transition. The feature on the right side of the spectrum corresponds to frequency that excites the  $4s_{1/2}$   $f=1$  to  $5p_{3/2}$  transition.

One final step to produce a large voltage change for small frequency shifts at the atomic transition frequency is called dithering. Dithering the laser frequency changes the laser frequency very slightly and rapidly ( $\approx 16$  kHz) to create a derivative signal. The derivative signal is zero at the Doppler-free feature, and its slope is very large (Red signal in Figure 7). An inherent problem of locking to a peak on the Doppler-free signal is that the voltage will decrease for a frequency change in either direction. The derivative signal resolves this issue, because near the peak it shifts from negative to positive, crossing zero at exactly at the peak. The signals in Figure 7 are obtained when the frequency of the laser is scanned. When this scanning is turned off, the correct frequency can be found by adjusting the frequency manually to arrive at the correct feature. That feature is the zero voltage point on the derivative signal corresponding to the  $4s_{1/2}$  to the  $5p_{3/2}$   $f=1$  transition labeled in Figure 7. For a stable frequency, the corresponding voltage will remain constant. The voltage can be fed into in a feedback circuit along with a set point voltage, where the difference is sent to the piezo driver that controls the diffraction grating. This setup stabilizes the frequency of the laser diode. Note that the 770 nm laser diode is stabilized in the same way, only driving the  $4s_{1/2}$  to  $4p_{1/2}$  transition.

## 2.5 Rydberg Excitement: Stage II

### 2.5.1 Setup

A 978 nm laser diode is used to excite atoms in the  $5p_{3/2}$  state to Rydberg states, such as the 40d state. The experimental arrangement for the 978 nm laser is given in Figure 8. Like the 405

nm laser, the beam passes through an optical isolator to prevent reflection of the beam from other optics components back into the laser diode cavity. A microscope slide reflects approximately 20% of the light into a Thorlabs Fabry Pérot interferometer to check for single mode lasing. Another microscope slide reflects some light into a MOGLabs MWM wavemeter. The wavemeter displays the wavelength of the light. It is precise to within 200 MHz (0.0004 nm) and accurate to within 600 MHz (0.001 nm) at 780 nm [18]. The wavemeter is useful for tuning the wavelength of the 978 nm laser to excite different Rydberg states that require different wavelengths. Another microscope slide passes the light into an optical fiber sent to an arrangement to lock the frequency of the laser diode. The remaining light is sent through an acousto-optic modulator to a fiber which goes to the magneto optical trap.

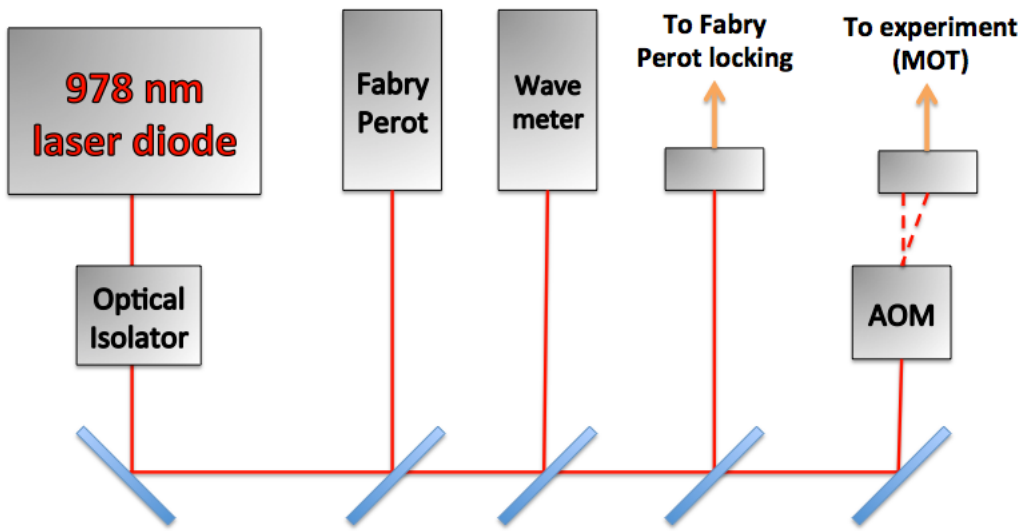


Figure 8: Top-level experimental setup for the second stage of Rydberg excitation. Photons from the 978 nm ECDL first pass through an optical isolator to prevent back reflection in the cavity. Light is reflected off of mirrors (leftmost and rightmost blue rectangles) and 20% reflective microscope slides (middle three blue rectangles) to pass light into various components. The Fabry Pérot is used to check if the laser color is a single frequency. Some light is directed to a different Fabry Pérot for frequency locking. Some goes to a MOGLabs wavemeter to monitor the wavelength of the light. The rest passes through an acousto-optic modulator to switch light on and off in the MOT.

### 2.5.2 Acousto-Optic Modulator

The acousto-optic modulator (AOM) acts as an ultrafast switch to turn on and off the 978 nm beam passing through the magneto-optical trap with a rise and fall time of approximately 100 ns each. The beam should pass through the MOT cloud for time intervals on the order of 1-100 microseconds. Simply turning the laser on and off is both slower, and problematic for frequency stabilization purposes. The AOM resolves both issues by using Bragg diffraction to align/misalign the beam into the fiber, rather than turning the laser on and off. An acousto-optic modulator uses a photon-phonon scattering process and acts as a tunable diffraction grating. The AOM contains a transparent crystal through which the light propagates. An rf signal is passed to a piezoelectric transducer in contact with the crystal, which generates a sound wave in the crystal. When a photon absorbs a phonon from the sound wave, a first order scattering process occurs. Photon and phonon momentum and energy conservation give the Bragg angle of diffraction for the photons,

$$\sin(\theta_B) = \frac{\kappa}{2k_i} \quad (3)$$

where  $\theta_B$  is the Bragg angle,  $\kappa$  is the phonon momentum, and  $k_i$  is the photon momentum. The photon momentum is  $k = \frac{\omega}{v_l}$  where  $\omega$  is the frequency of light and  $v_l$  is the speed of light in the crystal. The phonon momentum is  $\frac{\sigma}{v_s}$  where  $\sigma$  is the rf frequency and  $v_s$  is the speed of sound in the crystal [17].

When the rf signal is on, some light passes straight through the AOM (0th order), and some light is diffracted to the 1st order Bragg diffraction angle. The AOM can be adjusted so that only a very small amount of light is sent to other orders of the Bragg diffraction angle. When the rf signal is off, all of the light passes through the crystal to the 0th order location. By aligning the 978nm laser beam with the location of the 1st order Bragg angle, light will only enter the MOT when the rf signal is on. This setup makes maximizing the light diffracted to the first order Bragg angle important. The rf signal can be controlled at very high speeds for optimal switching into the MOT.

### 2.5.3 Frequency Stabilization: Scanning Transfer Cavity Lock

The blue laser could make use of a potassium vapor cell in the ground state to lock the frequency, because the transition begins in the ground state. Excitation from the  $5p_{3/2}$  state to the Rydberg states requires a more clever locking mechanism, because the  $5p_{3/2}$  state is not populated in a vapor cell.<sup>1</sup> The alternative method used in this experiment is called a scanning transfer cavity lock. The technique requires a stable reference laser at some other wavelength, and a Fabry-Pérot interferometer.

Previous studies of a transfer cavity lock technique with a Fabry Pérot interferometer show the system is adequate for stabilization of a laser diode for long periods of time. One group locked a laser diode that typically drifts about 50 MHz/h to within  $\pm 1.2$  MHz for many hours [16]. Another group also stabilized a laser to with  $\pm 1$  MHz/h [13]. Many groups have successfully used this technique to consistently create Rydberg atoms for many hours [15].

A Fabry-Pérot interferometer consists of two highly reflective concave mirrors (97% reflective) separated by a distance  $L$  (approximately 10 cm in this experiment) that share a focal point. For most wavelengths, incident light is reflected back and does not enter the cavity. The light must pass through the 97% reflective mirror twice, so very little light escapes the far mirror. However, certain wavelengths are resonant with the cavity. When the light traveling through the cavity travels the correct distance such that when it reaches the starting point, its wave is perfectly in phase with the incoming light, constructive interference occurs. The increased intensity of light in the cavity allows light to pass through the far mirror. The condition for constructive interference is  $m\lambda = 4L$ , where  $m$  is an integer,  $\lambda$  is the wavelength of light, and  $L$  is the distance between the mirrors. This can be visualized in Figure 9.

---

<sup>1</sup>While one could create a cell with some  $5p_{3/2}$  atoms, the  $5p_{3/2}$  to 40d transition is so weak there would not be a strong enough Doppler-free signal to lock to.

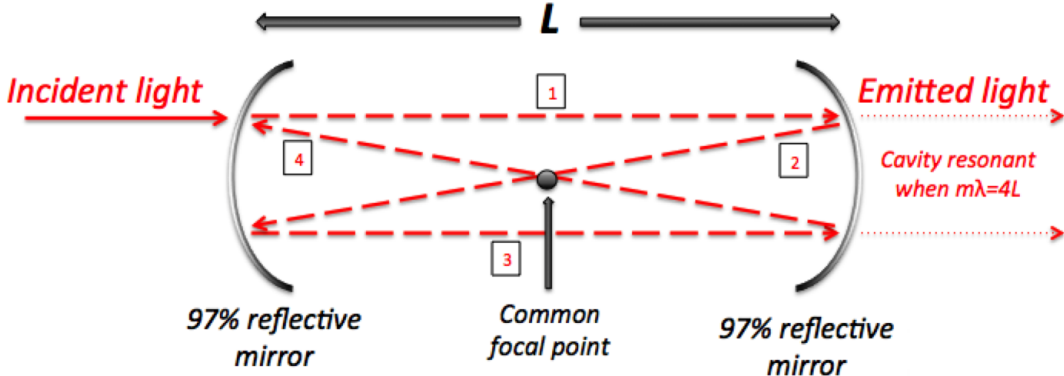


Figure 9: Theoretical diagram of the Fabry Pérot interferometer used in this experiment for the frequency locking of the 978 nm laser. It consists of two highly reflective mirrors (97% reflective) separated by a distance  $L$  (approximately 10 cm in this experiment). For most cavity lengths, light does not pass through both mirrors. For certain wavelengths, constructive interference occurs and light is emitted out of the right mirror. The condition for constructive interference is approximately  $m\lambda = 4L$ , where  $m$  is an integer,  $\lambda$  is the wavelength of light, and  $L$  is the distance between the mirrors. If light travels along the path denoted by 1, 2, 3, 4, and  $L$  is much greater than the height of the mirrors, then this condition makes sense.

Assuming the wavelength of the light is constant, light will pass through the cavity only when the two mirrors are certain quantized distances  $L$  apart. Now imagine one of the mirrors moves back and forth at some frequency, and the light exiting the cavity enters a photodiode that outputs a voltage proportional to the intensity of light. The photodiode will have a low output, and then show a narrow peak as the mirror passes through the resonant cavity distance. In this experiment, one of the mirrors is attached to a PZT (piezoelectric transducer), a small piece of ceramic that changes length when a voltage is applied to it. There is a specific voltage that makes the cavity resonant with the light. Applying a ramp voltage to the PZT moves the mirror back and forth at a constant rate, so a peak always appears at the same time after the start of the ramp. If the wavelength of the light shifts, the peak will shift in time as well.

The time difference between the ramp trigger and the peak can be converted to a DC voltage, and placed in a feedback loop with a PZT that adjusts the frequency of the laser diode. If the wavelength shifts due to atmospheric changes, the PZT on the diode will adjust the laser frequency to keep the peak in the same position, and keep the wavelength a constant. The problem with relying on this mechanism is that the cavity length is not necessarily stable over time. Thermal

expansion of the quartz between the mirrors, for instance, will cause the resonant frequency of the cavity to shift on the ramp, causing the frequency of a locked laser to shift as well.

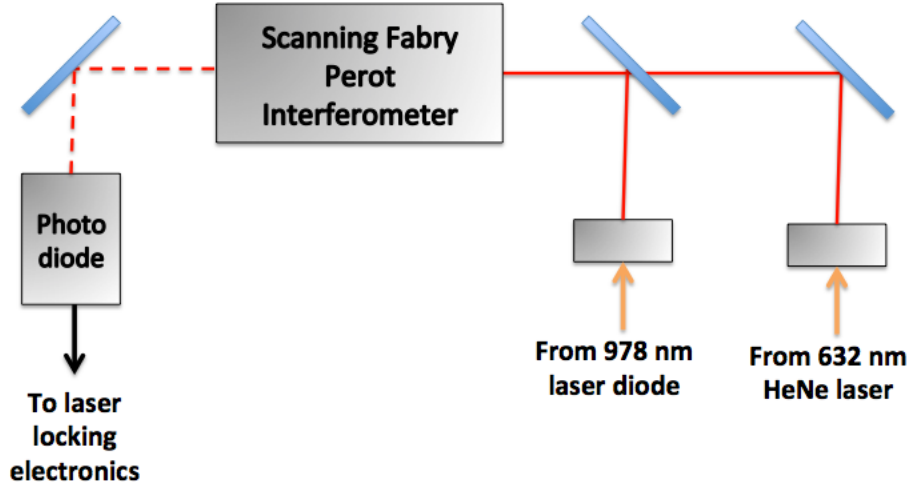


Figure 10: Experimental layout for the scanning transfer cavity locking setup. Light from the 978 nm laser and the stable Helium Neon reference laser pass through the scanning Fabry P  rot interferometer. The light is collected by the photodiode. The resulting signal outputted by the photodiode is given in Figure 11

The solution is to lock the length of the Fabry P  rot cavity to a reference laser that is stable under atmospheric conditions. A stabilized HeNe laser radiates light at 632.8 nm, stable to within  $\pm 2$  MHz. Placing the Fabry P  rot cavity length (piezo voltage) in electronic feedback with the location of the stable Helium Neon peak will prevent the cavity length from drifting. The unstable 978 nm laser is simultaneously aimed into the stable Fabry P  rot cavity (Figure 10). The 978 nm creates its own set of distinct peaks because its wavelength is resonant with the cavity at different cavity lengths than the 632 nm laser. The same electronic circuit creates a DC voltage signal proportional to the time difference between the first peak (HeNe) and the second peak (978 nm laser diode). This voltage is placed in a feedback loop with the diffraction grating on the 978 nm laser diode to stabilize its frequency. See Figure 11 for an oscilloscope signal containing the piezo voltage, and two peaks for the different wavelengths.

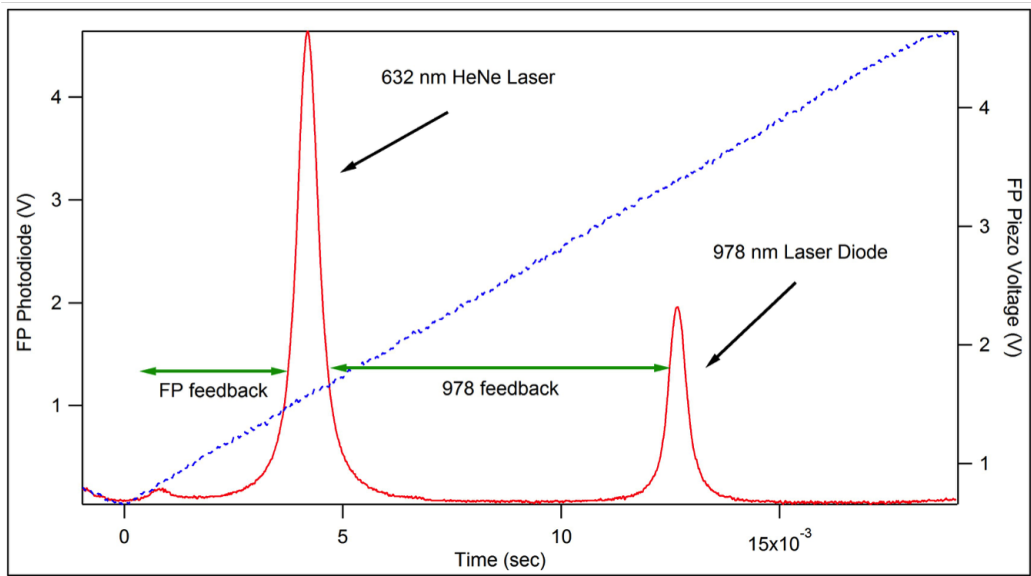


Figure 11: The blue signal (right axis) is the ramp voltage applied to the piezoelectric transducer attached to one of the mirrors on the Fabry Pérot interferometer. The length of the cavity changes with the voltage (though not necessarily linearly). The red signal (left axis) is the signal from the photodiode in Figure 10. The 632 nm laser and 978 nm laser are resonant with the cavity at different distances, so they emit light at different times. The time between the start of the ramp and the first peak is used to lock the Fabry Pérot cavity, and the time between the two peaks is used to lock the frequency of the 978 nm laser.

The electronic locking circuit has been designed to work such that the 632 nm peak should come before the 978 nm peak. It is just as likely, however, that the frequency resonant with the transition will make a peak that comes before the 632 nm peak. It is necessary to have some way to adjust the location of the peaks without altering laser frequencies. The solution is a pump and a needle valve that controls the pressure inside the pressure sealed cavity. The index of refraction of air depends on pressure, and slightly on the frequency of light. The wavelength  $\lambda$  of light in a medium depends on the index of refraction  $n$  and the wavelength of the light in a vacuum  $\lambda_{vac}$  by  $\lambda = n\lambda_{vac}$ . Note that adjusting the wavelength will not change the frequency of the laser, which is the important parameter for exciting electrons. Changes in wavelength change the peak location, and since the peaks do not move together, their relative positions change. It is easy to adjust pressure until a HeNe peak is positioned before a 978 nm laser diode peak.

## 2.6 Rydberg State Detection

Once Rydberg atoms have been made, it is necessary to have some mechanism of detecting them, and the state they are in. This experiment uses a strong electric field to ionize electrons from Rydberg atoms, and detects the electrons with an amplified signal produced by microchannel plate detectors. The large dipole moment of Rydberg atoms makes them very sensitive to external electric fields. Applying reasonable laboratory scale electric fields can allow an electron to break free from a Rydberg atom and be detected by the electron detector.

### 2.6.1 Field Ionization

The classical Rydberg atom model with one electron far from the positively charged inner shell is useful when considering its electric potential. The Coulomb potential of a hydrogen atom in 1-D is

$$V = -\frac{ke}{|z|} \quad (4)$$

where  $z$  is the distance from the nucleus in terms of Bohr radii, is a very good approximation for the electric potential of a Rydberg atom. The potential binds electrons with energy lower than that of the maximum value of the potential (Figure 12). Applying an external electric field of magnitude  $E$  and potential energy  $V = -Ez$  tilts the electric potential of the system. The new electric potential is given by the sum of the two electric potentials. Electrons in states with energy higher than the new electric potential boundary escape the electric potential of the atom and become ionized (Figure 12). Tuning the external electric field can selectively ionize states. In Figure 12, state 1 remains bound by the electric potential, while state 2 is ionized. Rydberg atoms have their energy states spaced nicely, so selective detection of Rydberg states is quite feasible. Once the electron is free, the electric field accelerates the electron towards the detector.

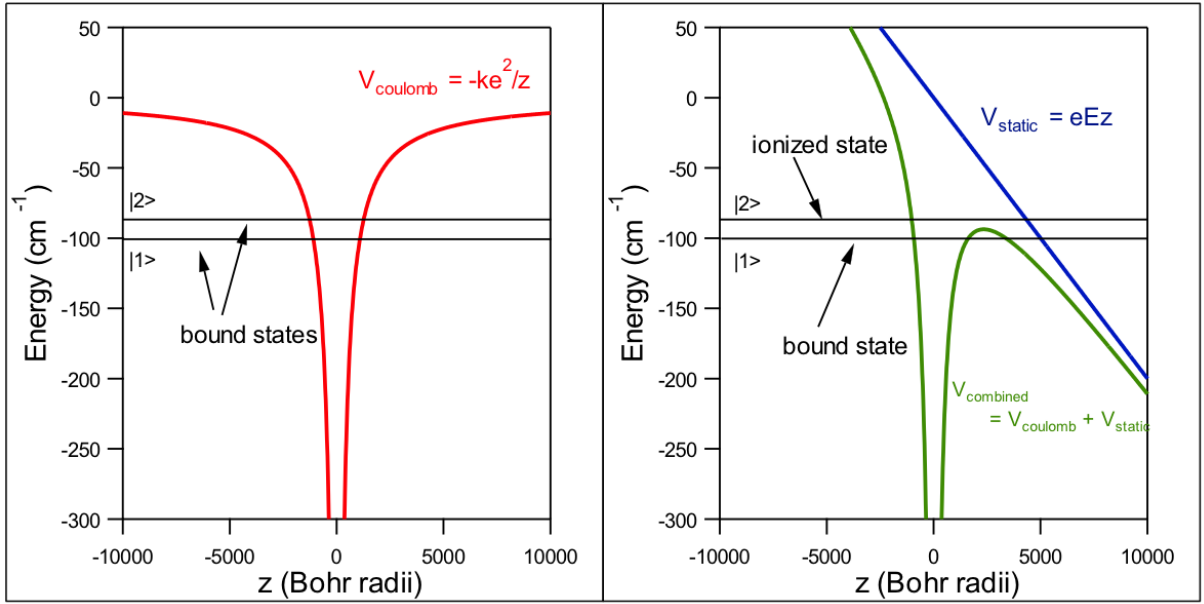


Figure 12: The potential energy for a Rydberg atom, approximated by the coulomb potential (left). The potential energy for a static electric field (right, blue), and for the sum of the coulomb potential and an external electric field (right, green). Electrons are ionized when their energies are greater than the energies bounded by the potential. Electrons from different Rydberg states can be selectively ionized by changing the magnitude of the external electric field. Figure courtesy of Dr. Charles Conover.

The electric field  $E_{FI}$  required to ionize an electron in a Rydberg atom is proportional to  $r^{-2}$ , or  $n^{-4}$  [1]. The 40d state in potassium requires an electric field of 132 V/cm to ionize the valence electron. The electric field is produced using 4 conducting metal rods inside of the vacuum chamber of the magneto-optical trap. A ground voltage is applied to the two rods closest to the electron detector, and a large negative voltage is applied to the two rods furthest from the electron detector. The rods produce an electric field with a gradient of approximately 1% at the center of the MOT cloud. The electric field is proportional to the difference in electric potential of the rods  $E_{FI} \approx 0.2273 * \Delta V$ . Applying a voltage of at least 580.7 V/cm should produce a field that just ionizes electrons in the 40d state. The voltages on the rods are controlled by a short current pulse through a trigger transformer. A primary voltage of 20 V DC produces a secondary voltage of about 600 V DC on the conducting rods.

### **2.6.2 Microchannel Plate Detector**

The electric field that ionizes the Rydberg atoms points from the grounded conductors to the negative potential conductors, or away from the electron detector. Once ionized, the free negatively charged electrons are accelerated in the opposite direction of the field, or towards the electron detector. A microchannel plate detector amplifies the signal produced by a single electron. Microchannel plates are electron multipliers with a very high gain. The microchannel plate consists of millions of glass channels with a very small diameter arranged in a 2D array (Figure 13). The array extends back about 1 mm. An incident electron enters one of the channels and strikes the glass channel wall, which releases a secondary electron [14]. Placing a potential difference of 1000 V across the two ends of the microchannel plate produces a strong electric field that accelerates both electrons down the channel. The electrons travel in a parabolic shape until they again collide with a channel wall, releasing more secondary electrons. This process cascades down the 1 mm long tube until about  $10^3$  electrons exit the back of the plate. In this experiment, a second microchannel plate is placed behind the first, yielding  $10^6$  electrons after the second plate from just the single initial electron. The output electrons are collected by a steel plate and produce a current (Figure 13). This current is converted to a voltage that is outputted to the oscilloscope. When no Rydberg atoms are present and no electrons ionized, random fluctuations occur on the electron detector signal due to random thermal excitations within the microchannel plates (“dark currents”). These excitations can occur anywhere along the length of a channel at any time, so the magnitude and timing of these signals are random (typically about 1000 occurrences per second). When Rydberg atoms have been produced, a large and consistent voltage drop appears on the detector that is easily distinguished from these fluctuations.

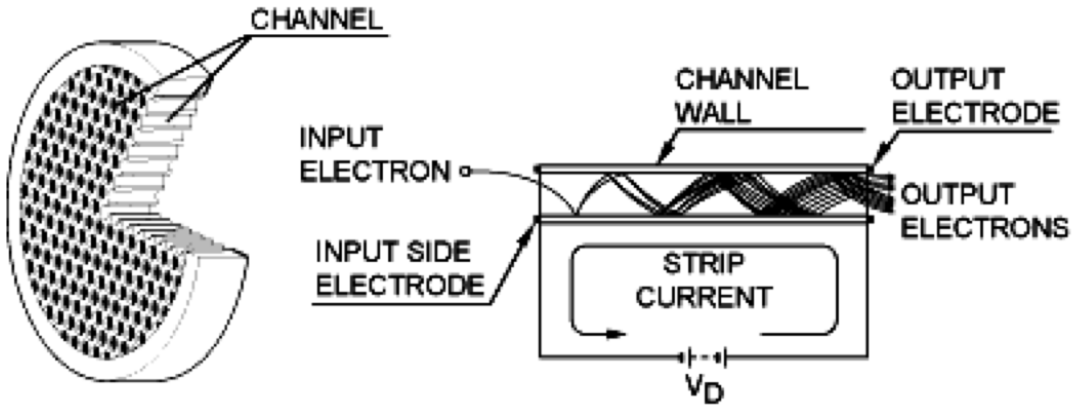


Figure 13: Diagram of a microchannel plate detector. Electrons enter a 2D array of tiny glass channels, and multiply as they are accelerated down the channel by a large potential difference. Output electrons are converted to a current by a steel plate. Image taken from [14].

The 1000V potential difference applied across the two 1 mm microchannel plates produces a field that is mostly confined to the region between the plates, similar to a capacitor. However, despite a shield, stray electric fields are present which result in imperfections in the electric field in the center of the MOT that deviate from the field calculated from the orientation of the rods. The field has an uncharacterized gradient across the MOT. The energy levels of potassium atoms in the MOT become Stark shifted from the stray electric field, even when no voltage is applied to the conducting rods.

There are two timing parameters that are important for detecting Rydberg atoms. The first controls the acousto-optic modulator that switches the 978 nm laser diode into the MOT. The second controls the field ionization pulse that ionizes electrons and accelerates them towards the microchannel plate detectors.

## 2.7 Resonant Collisions

Resonant collisions are energy transfers that occur when atom A gains as much internal energy as atom B loses. In ultra-cold Rydberg atoms, these are not physical collisions, but rather quantum mechanical energy exchanges due to the strong dipole-dipole interactions of Rydberg atoms. Typically, these resonant energy exchanges can occur due to accidental equalities in energy spacings. That is, of the thousands of energy levels that exist across all different atoms, two energy levels

just happen to be spaced such that  $\Delta E_{atom1} = -\Delta E_{atom2}$ .<sup>2</sup>

A far more likely occurrence than these exact accidental energy spacings are near resonant energy spacings. Energy would almost be conserved in such an exchange, but not quite, so it is very unlikely an energy transfer occurs without the assistance of kinetic energy. However, as we saw in the section on Stark shifting, energy levels can be finely tuned with external electric fields. Rydberg atoms are particularly sensitive to external electric fields, so only moderate electric fields (on the order of 10 V/cm) are required to bring the atoms into resonance. Consider two potassium atoms, both in the Rydberg state 40d. The energy levels of potassium near this state as a function of electric field are given in Figure 14. Different orbital angular momentum states respond differently to electric fields. For instance, the energy of atoms in the 40d states drops more rapidly than the energy of atoms in the 40p states.

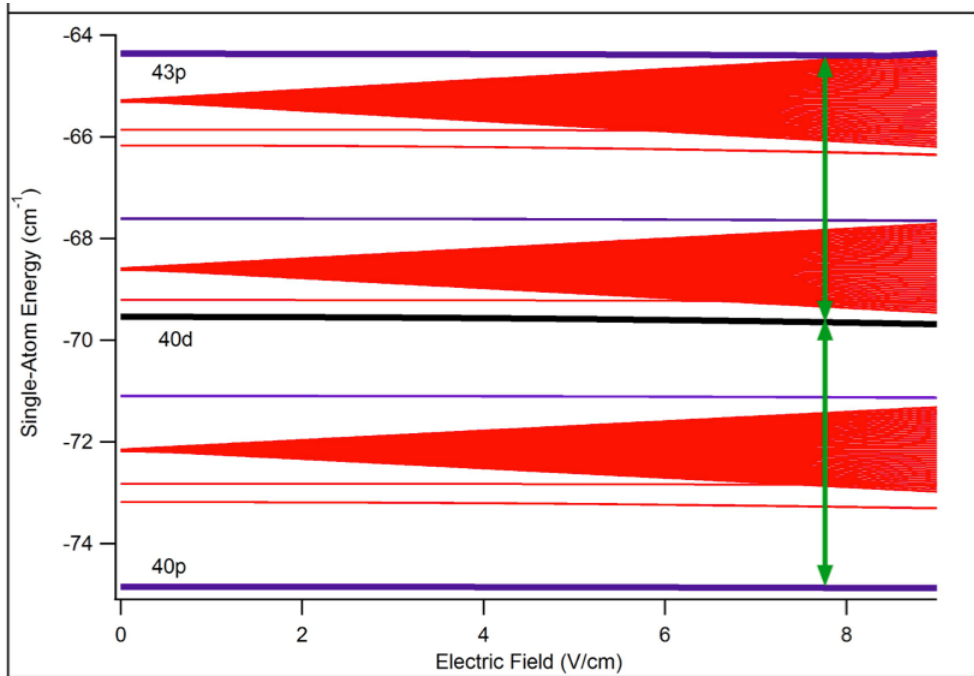


Figure 14: Single atom energy levels for potassium atoms with  $n=40$  as a function of electric field. Stark shifts are calculated numerically. The black line corresponds to an atom in the initial 40d state. The thick purple lines correspond to the 40p and 43p states. When the two purple lines are equidistant to the black line, denoted by the green arrows, resonant collisions have a higher probability of occurring. The red lines are from many high angular momentum states that are degenerate at zero electric field, but spread out as the field increases.

<sup>2</sup>This type of resonant exchange is what drives the Helium Neon laser used for the Fabry Pérot stabilization. It is so stable because its frequency references an atomic transition.

This can be more easily visualized by looking at the sum of energies of two atoms. In Figure 15, the y-axis is the combined energy of two atoms in a few states relevant to this discussion, while the x-axis is again the electric field in V/cm. A pair of 40d potassium atoms will decrease in energy with an increasing electric field. At some electric field strength, approximately 8 V/cm in this case, the combined energy of the two 40d atoms is the same as the combined energy of one atom in the 40p state, and one atom in the 43p state. The pair of atoms then has an increased probability of a resonant energy transfer, where one of the 40d atoms gains energy from the other atom and moves into the 43p state, while the atom that shared its energy drops to the 40p state. In a population of 40d atoms at this electric field, the number of atoms in each state will evolve in time depending on how strong the resonant collision is, and how close the energy levels are to resonance.

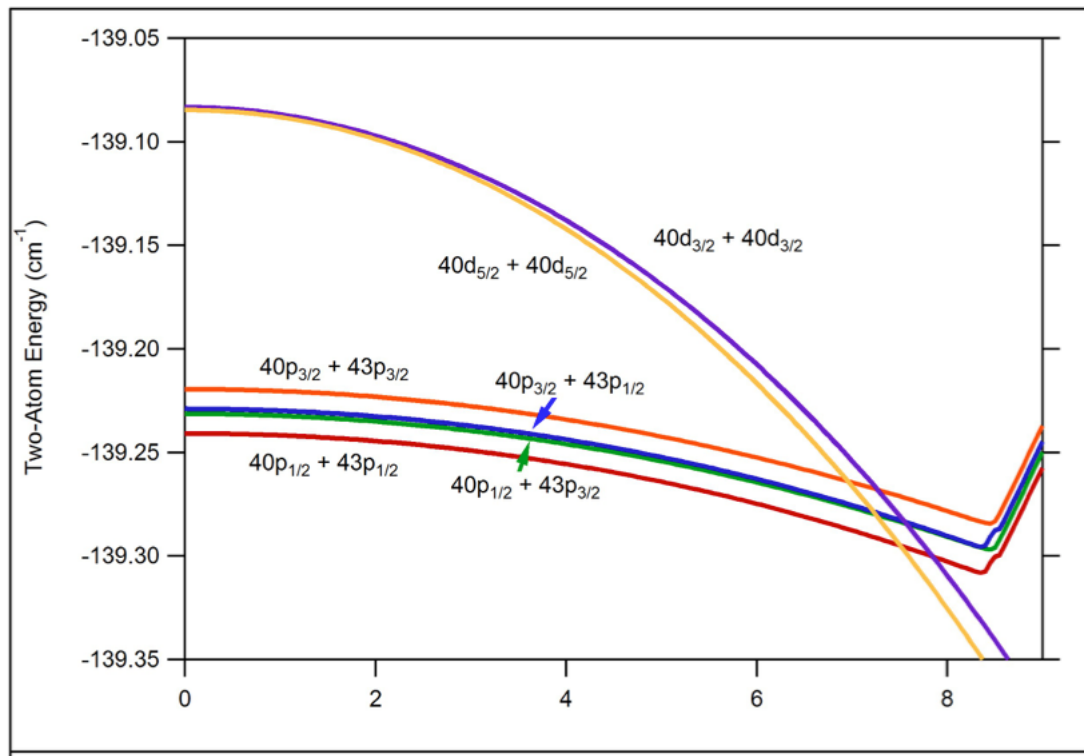


Figure 15: The sum of the energies of selected pairs of atomic states in potassium as a function of electric field. When an electric field is selected such that the energy of a pair of 40d atoms has the same energy as a 40p atom and a 43p atom, resonant energy transfers can occur between two closely spaced 40d atoms to produce a pair of 40p and 43p atoms. This occurs between 7 and 8 V/cm in this example.

In order to induce resonant collisions, an additional experimental step must be added to the Rydberg atom creation and detection experiment. After the AOM has been turned off to prevent the 978 nm laser from hitting the MOT cloud, and before the field ionization pulse, another electric field is applied inside the MOT cloud. This electric field is also applied by applying a voltage to the conducting rods in the MOT, though the voltages are much smaller than those used to create the field ionization pulse.<sup>3</sup> When the correct voltage is applied to the rods, the extra electric field tunes the Rydberg atoms into resonance, and resonant collisions should occur. After this electric field pulse, which is on the order of one microsecond in length, there should be some combination of 40p, 43p, and 40d Rydberg atoms in the MOT cloud. Then the large field ionization pulse is applied. Since the field ionization pulse takes about half a microsecond to ramp up to its maximum value, atoms with lower ionization energy will release their electrons first, at a lower electric field magnitude. These different ionization times should be distinguishable as three different peaks on the microchannel plate detector. In this case, the 43p peak will come first, then the 40d peak, and finally the 40p, in decreasing order of energy. This process is visually summarized in Figure 16.

---

<sup>3</sup>A positive voltage between 0 and 10 V is applied to the two conducting rods closest to the electron detector. A constant negative voltage of about -20 V is applied to the two conducting rods furthest from the electron detector, because the box that controls the voltage on the positive rods during the experiment can only ramp between 0 and 10 V. The negative offset voltage is used to get the electric field in range of the electric field where resonant collisions are expected, and the positive voltage is changed from run to run to scan over electric fields close to this value.

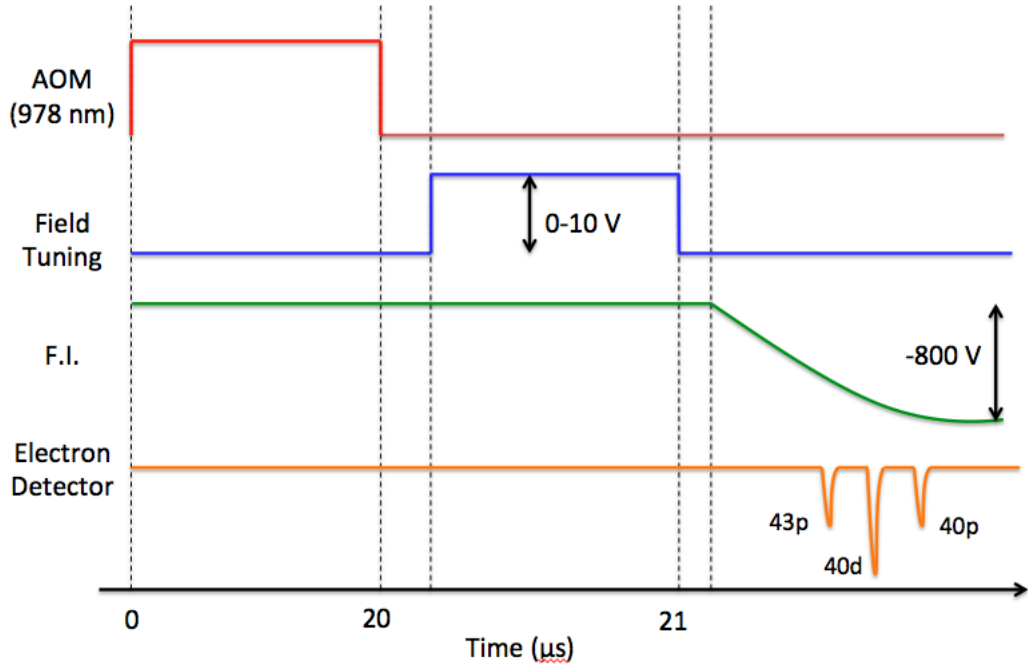


Figure 16: Timing schematic to induce resonant collisions. Exact times in  $\mu s$  can be changed from run to run, if desired. The 978 nm laser creates Rydberg atoms for 20  $\mu s$ , until it is turned off by turning off the AOM (blue). A small positive electric potential (between 0 and 10 V) is applied to the conducting rods closest to the electron detector (red). This field brings the energies of the 40d Rydberg atoms close to resonance. The small field is turned off and replaced with a very large ionizing electric field created by the -800V on the far conducting rods (green). Since the ionization field takes about half of a microsecond to ramp up, the 43p, 40d, and 40p Rydberg atoms will have their valence electron ionized and detected by the electron detector at different times (orange).

## 3 Results and Discussion

### 3.1 Scanning Transfer Cavity Lock Frequency Stabilization

The scanning transfer cavity lock setup was initially tested using a 770 nm laser. While the scanning transfer cavity lock is used for the 978 nm laser in the experiment, both laser diodes are constructed in the same way, so there is no reason to think results should vary drastically based on wavelength (particularly since the Fabry Pérot is in a sealed cell with a constant pressure). The 770 nm laser drives the  $4s_{1/2}$  to  $4p_{1/2}$  transition, and was chosen because this transition references the ground state. The transition also has resolvable ground state and excited state hyperfine structure, which is useful for calculating frequency drift. Monitoring the absorption signal on a potassium vapor cell provides another external measurement of frequency drift to determine the efficacy of the scanning transfer cavity lock. The laser frequency is scanned over the crossover peak of the Doppler-free absorption signal (Figure 17). The cross over peak was chosen because it contains the sharpest features. There are three separate peaks on the cross over peak because the  $4s_{1/2}$  and  $4p_{1/2}$  both have  $f=1$  and  $f=2$  states. The middle peak is an excited state crossover peak. The frequency difference between the  $4p_{1/2}$   $f=1$  and  $4p_{1/2}$   $f=2$  states is 55 MHz, which gives a frequency scale between the left and right absorption dips. Calculating frequency drift based on a feature on the the Doppler-free signal is problematic, because the the signal can shift up and down based on temperature (and associated vapor pressure) changes within the potassium vapor cell, or changes in intensity of the laser. The minimum of the peaks, however, do not shift in frequency location (though they may shift up and down). To take advantage of this, a derivative of the absorption signal is taken by dithering the laser current (Figure 17). The minimum corresponds to a zero on the derivative signal, and does not shift with temperature or intensity changes. The zero of the right most peak is chosen as the frequency which the 770 nm laser is locked to. The frequency scale from the known 55 MHz distance can be used to calculate the frequency difference between the local minimum and maximum about the lock point, which turns out to be 7.5 MHz. Using the voltage of the minimum and maximum (which varies from run to run), a slope in V/MHz can be calculated to use a conversion factor from a voltage drift on the photodiode to a frequency drift on the 770 nm laser.

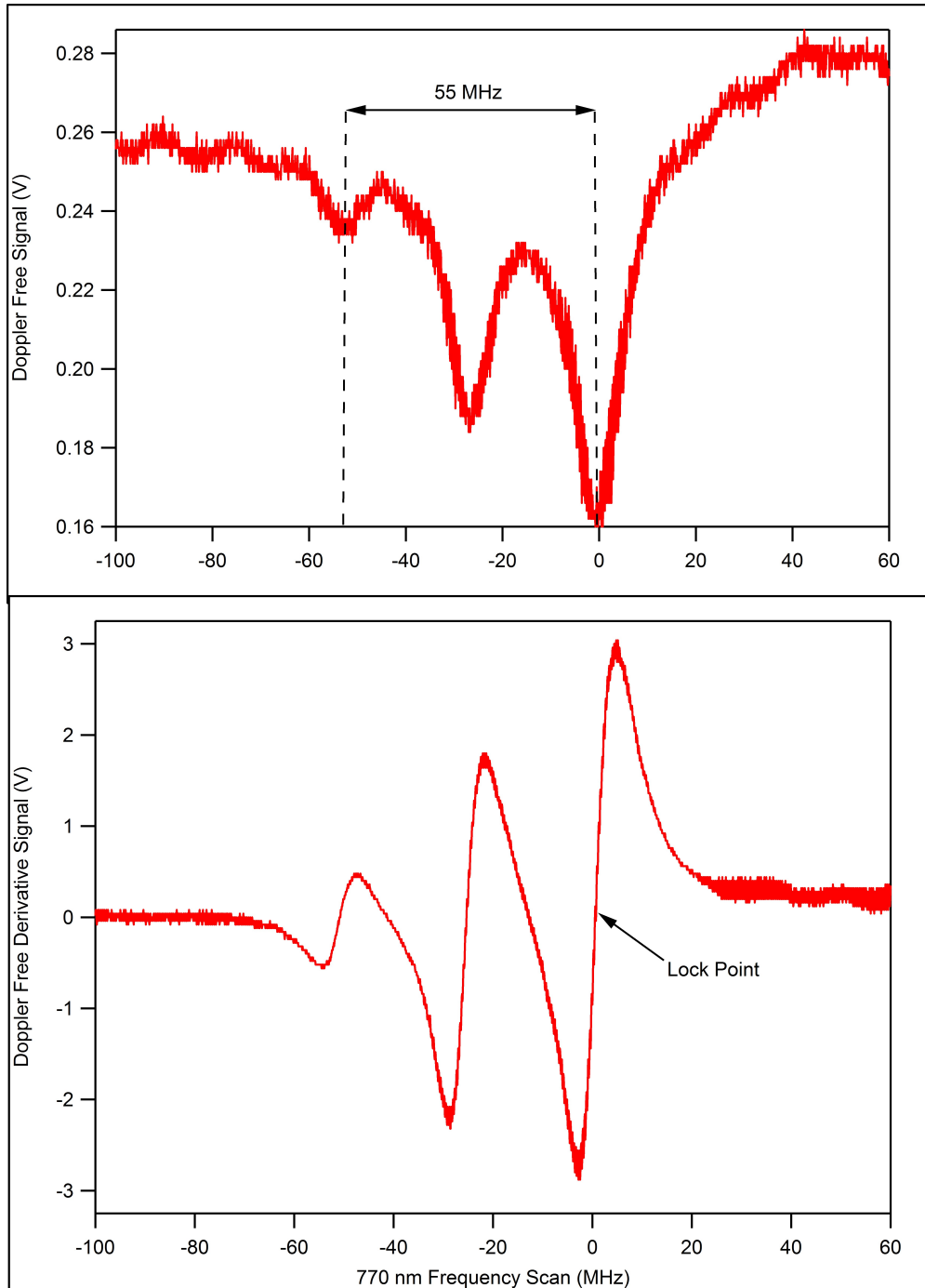


Figure 17: (Top) Doppler free spectroscopy signal of a 770 nm laser scanned over the  $4s_{1/2}$  to  $4p_{1/2}$  transition. Only the crossover peak is shown here. The frequency difference between the  $4p_{3/2}$   $f=1$  and  $4p_{1/2}$   $f=2$  states of 55 MHz provides a frequency scale for the signal. (Bottom) The derivative of this doppler free signal. The frequency of the laser is locked to a frequency that initially corresponds to the zero point of the right feature (or minimum of the Doppler-free signal).

A set of data showing the frequency of the 770 nm laser calculated from this absorption signal over a 20-minute time period is given in Figure 18. The frequency varies within a  $\pm 3$  MHz window over the entire 20-minute scan. The true frequency of the laser is approximately 400,000 GHz, so this stabilization is to one part in  $10^8$ . The stabilization is comparable to the stabilization seen by similar experiments of  $\pm 1$  MHz [13]. The true test of the adequacy of this level of stabilization for the creation of Rydberg atoms came from the Rydberg experiment itself. We found that we could excite Rydberg atoms for a few hours, without having any problems with frequency drift in the 978 nm laser diode. Experimental failure typically came as a result of failure in the frequency lock of the 405 nm laser diode on timescales of about 30 minutes, although we believe these problems are not a result of the locking mechanism, but the laser diode itself.

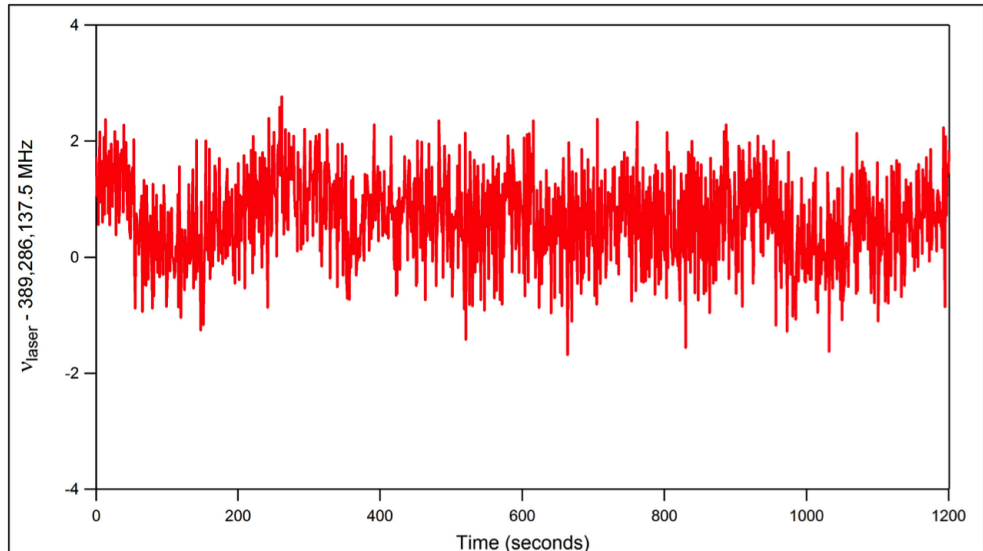


Figure 18: Frequency of the 770 nm laser stabilized by the scanning transfer cavity lock versus time in seconds. The frequency is stable to within  $\pm 3$  MHz over 20 minutes.

### 3.2 Rydberg State Detection

Figure 19 shows the photodiode signal of the 978 nm laser behind the MOT cloud in blue. The 978 nm laser is on for  $20 \mu s$  to produce Rydberg atoms until the AOM is turned off. A field ionization pulse of 800 V is applied for  $0.5 \mu s$  a short time after the AOM has been turned off. The electron detector signal in red in Figure 19 has a sharp dip in voltage after this field ionization pulse, which indicates electrons have been ionized and detected by the detector. The sharp dip is

absent when either the 405 nm laser or the 978 nm laser are off, indicating the ionized electrons came from Rydberg atoms.

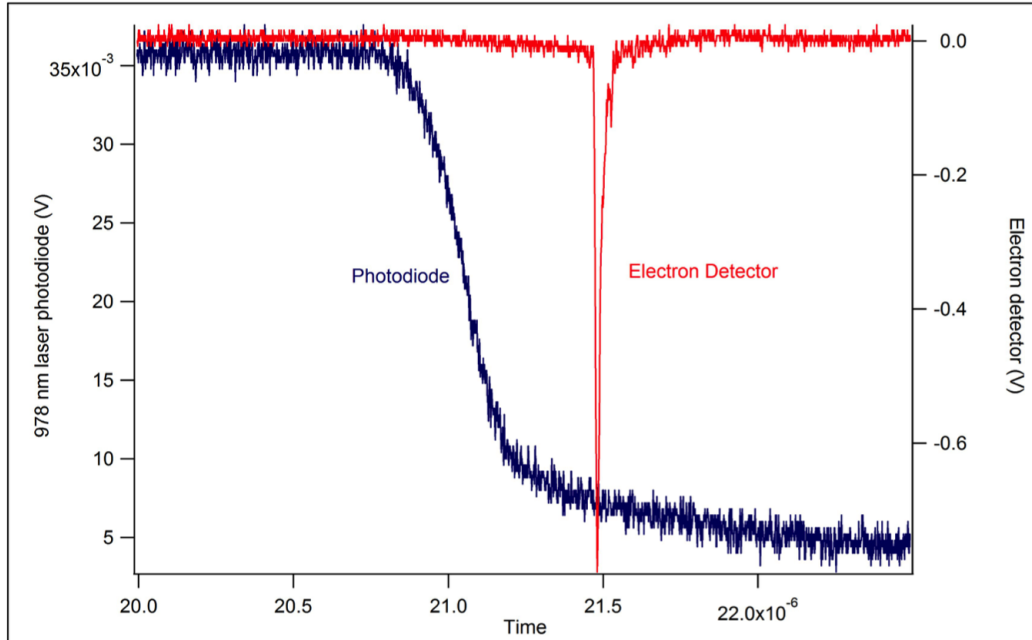


Figure 19: Photodiode signal of the 978 nm laser (blue, left axis). When the laser is turned off, the field ionization pulse is applied. Some time later, electrons are detected by the electron detector (red, right axis). The sharp peak indicates electrons ionized from Rydberg atoms. Such a peak does not occur without the 405 nm laser and the 978 nm laser exciting Rydberg states.

The exact wavelength of the laser at the time of this experiment according to the MOGLabs wavemeter was 978.465 nm. According to energy levels of potassium tabulated by the NIST Atomic Spectra Database, the wavelength needed to drive the  $5p_{3/2}$  to  $40d_{5/2}$  transition in potassium is 978.461 nm. One reason for this small discrepancy is a stray electric field at the MOT cloud due to the microchannel plate detector. The Stark shifts that would arise from such an electric field, however, seem too small to produce the wavelength difference observed here. Another possibility is a poor calibration of the MOGLabs wavemeter. This is also unlikely, because the wavemeter was calibrated with a Bureligh wavemeter, which has been very accurate in previous experiments. The wavemeter does also not show day-to-day drift, based on empirical observation. A final possibility is the data from the NIST Atomic Spectra Database is incorrect on one of the two energy levels involved in the transition.

### 3.3 Resonant Collisions

An experiment to observe resonant collisions is described in the resonant collisions section of the experimental overview. The electron detector never showed 3 peaks corresponding to the 40d, 40p and 43p Rydberg states as shown in Figure 16. Only a single peak was observed corresponding to the 40d Rydberg atoms, identical to the signal seen in the previous section on Rydberg detection. We conclude then that we were either unable to induce resonant collisions, or unable to induce enough resonant collisions such that they produce a signal on the electron detector that is distinguishable from the noise. Our leading hypothesis for this result is that the density of Rydberg atoms in the MOT cloud is too low. The dipole-dipole interactions that allow resonant collisions to occur decrease in strength as  $r^6$ . Increasing the density of Rydberg atoms in the cloud increases the likelihood two atoms are very close together and should increase the number of resonant collisions. The first series of approaches involved adjustments to the 978 nm laser. First, the beam was adjusted so that its focus (where the beam is narrowest) occurs at the MOT cloud. The beam diameter was narrowed from 1 mm to 0.1 mm, a 100x increase in the intensity of light. A narrower beam diameter does not change the laser power, so it should excite same number of Rydberg atoms in a smaller area, increasing density. The experiment done with the narrower beam diameter still did not produce resonant collisions.

The next logical modification to the 978 nm laser setup would be to increase the effective laser power going into the MOT cloud. The external cavity diode laser produces 12 mW of power. There are significant losses before the beam reaches the cavity, resulting in only 0.5 mW of power going into the MOT cloud. Each of the three microscope slides has a 10% loss for each face of the slide directed to other components such as the wavemeter (See Figure 8). The beam clips the sides of the AOM, resulting in another loss of 50%. Aligning light through the fiber coupler and into the fiber optic cable also leads to a 50% loss. Eliminating some loss from the microscope slides by rearranging the setup in Figure 8 would bring more light into the MOT. These improvements are ongoing.

### 3.4 Stark Shifts

While we were unable to detect resonant collisions, we gathered some other data demonstrating Stark shifts. The frequency of the 978 nm laser was scanned across the  $40d_{3/2}$  and the  $40d_{5/2}$  states.

The area under the Rydberg peak signal was monitored on the microchannel plate detector with an SRS250 boxcar integrator. The area, which is proportional to the number of Rydberg atoms detected at any given frequency, is plotted versus frequency in Figure 20. The experiment was done for six different electric fields applied at the same time as the Rydberg atoms are being excited. The frequency of the laser must be shifted for each run, so only the relative frequencies of the 40d Rydberg states are considered in this experiment.

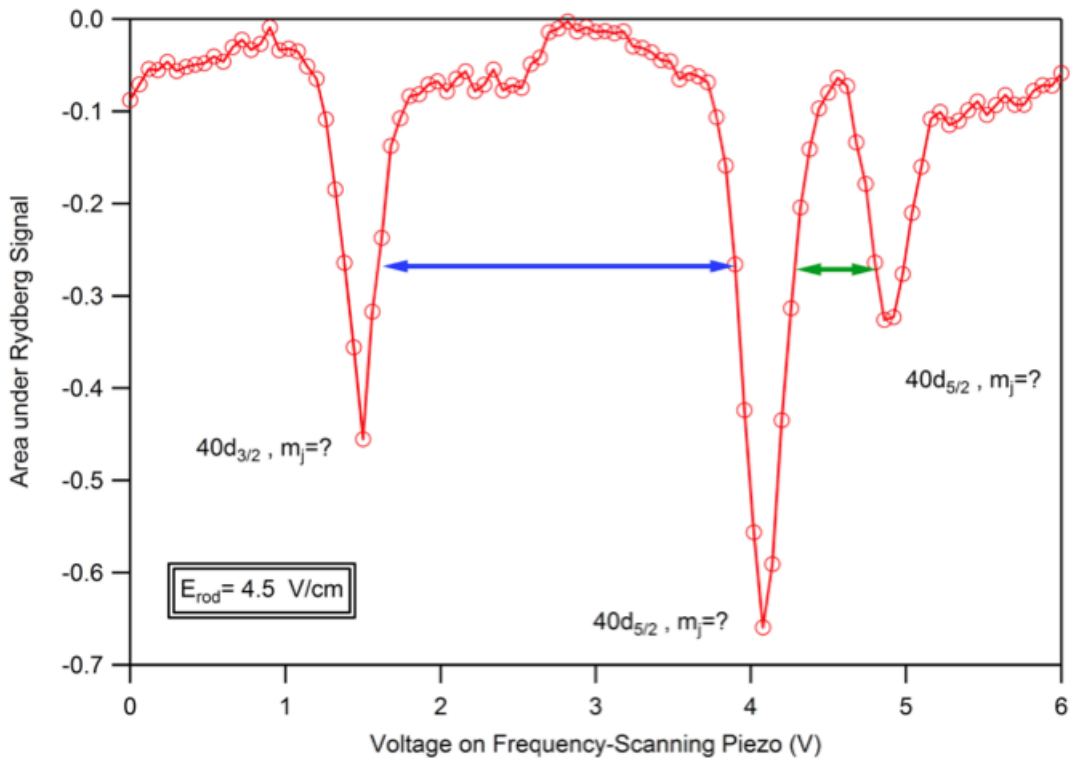


Figure 20: The frequency of the 978 nm laser scanned across the frequencies needed to excite the  $40d_{3/2}$  and the  $40d_{5/2}$  states. The area under the Rydberg peak signal was monitored on the microchannel plate detector with an SRS250 boxcar integrator, and plotted here as a function of voltage on the frequency scanning piezo. Only three Rydberg states are detected, although five are theoretically expected. The time difference between the first two peaks (blue) and second and third peak (green) are monitored for use in Figure 21.

With zero electric field, only two peaks should be visible from the  $40d_{3/2}$  and the  $40d_{5/2}$  states, because all of the  $|m_j|$  states are degenerate. At all other electric fields, there should be a splitting of the  $40d_{3/2}$  states into  $|m_j|=1/2$ , and  $3/2$ , and a splitting of the  $40d_{5/2}$  state into  $|m_j|=1/2$ ,  $3/2$ , and  $5/2$ . The positive and negative  $m_j$  levels are degenerate in electric fields, but not magnetic

fields. Figure 20 is the plot for an electric field of 4.5 V/cm. There are only three peaks rather than the expected five peaks. This finding is consistent across other electric fields. The frequency was scanned across frequencies much lower and higher than those shown in the plot, so no peaks were ‘missed’. The reason for this finding is a mystery. Perhaps there are two other peaks, but they are absorbed into one of the peaks shown, or they are just very small and are lost in the noise.

The frequency difference between the peaks for each electric field is plotted in Figure 21. Frequency differences were calculated from a combination of voltage on the frequency-scanning PZT, and the drift in the peak position of the 978 nm laser on the Fabry Pérot. One free spectral range, the frequency difference between two peaks on the Fabry Pérot, is 750 MHz for the cavity used in this experiment.<sup>4</sup> By measuring the distance a peak must travel on the oscilloscope to cover a free spectral range, an approximate frequency scale can be implemented to interpolate frequency shifts from peak shifts during the frequency scan in this experiment. These frequency estimates are good to about 10% and are given on the y-axis in Figure 21. Electric fields are calculated from the voltage on the conducting rods. An empirically determined offset in voltage was applied to each value to account for the stray electric field from the microchannel plate detector. The offset was chosen such that zero electric field would create zero frequency difference between the two  $40d_{5/2}$  peaks, because the states should be degenerate. Stark shifted energies for d states in Rydberg atoms are proportional to the square of the electric field. Figure 21 shows a linear relationship between the frequency differences and the square of the electric field, so the experimental frequency differences match the theoretical prediction.

---

<sup>4</sup>The free spectral range (FSR) of the Fabry-Pérot Interferometer can be calculated with the equation  $FSR = \frac{c}{4nL}$ , where c is the speed of light in a vacuum ( $3.000 \times 10^8 m/s$ ), n is the index of refraction ( $\approx 1$ ), and L is the distance between the two mirrors ( $\approx 10 cm$ ). The free spectral range is then 750.0 MHz.

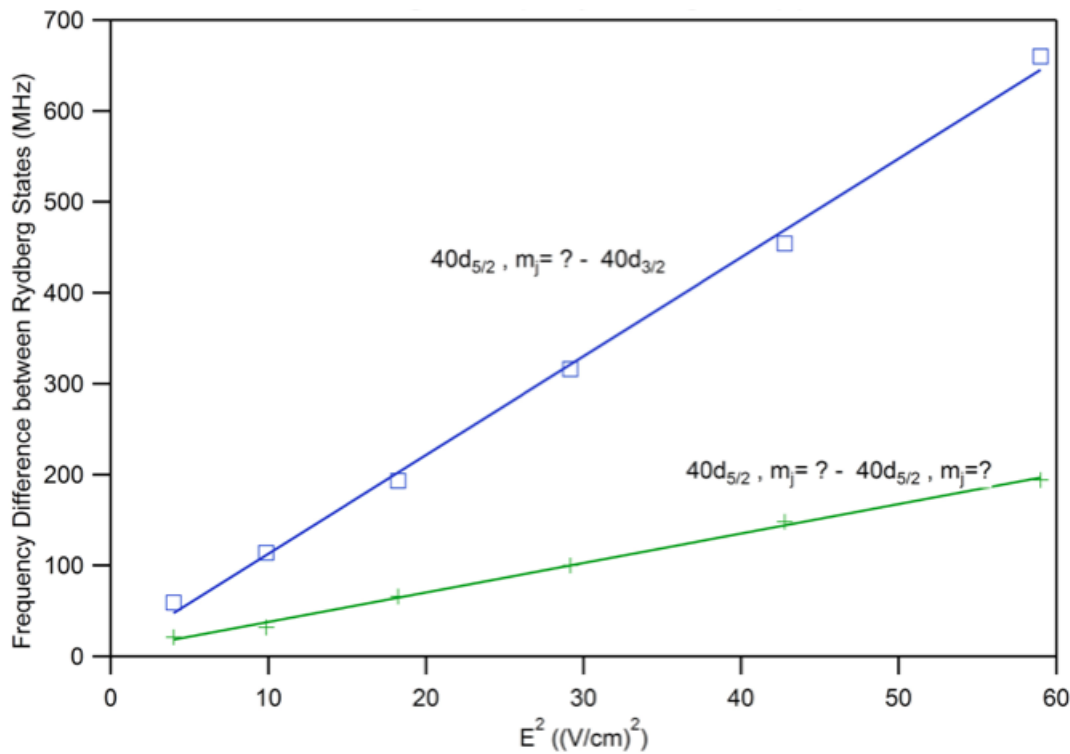


Figure 21: The frequency difference between the peaks from Figure 20 as a function of  $E^2$ . The blue line corresponds to the blue arrow frequency difference in Figure 20, and the green line corresponds to the green arrow frequency difference in Figure 20. Frequency differences were calculated from voltages on the frequency-scanning piezo and the peak positions on the Fabry Pérot interferometer. The linear relationship between Stark shifts and  $E^2$  matches theoretical predictions.

## 4 Conclusion

We were able to stabilize the frequency of the 770 nm laser diode to within  $\pm 3$  MHz over a course of 20 minutes with the scanning transfer cavity lock system. This technique was successful in stabilizing the 978 nm laser as well, confirmed by the successful creation and detection of Rydberg atoms for long periods of time. While resonant collisions were not observed, the successful creation of potassium Rydberg atoms was a big step towards the goal. The experiment in place should be able to induce resonant collisions with adjustments to Rydberg atom density in the MOT cloud.

## References

- [1] Gallagher, Thomas F. *Rydberg atoms*. Cambridge University Press, 1994.
- [2] Reetz-Lamour, M., Amthor, T., Deiglmayr, J., Westermann, S., Singer, K., Oliviera, A., Gustavo, L., Weidmüller, Mat., and Weidmüller, Mar., “Prospects of UltraCold Rydberg Gases for Quantum Information Processing”, Ed. Schleich, Wolfgang P., and Herbert Walther. *Elements of quantum information*. John Wiley & Sons, 2007.
- [3] Yin, Zhang-qi, and Fu-li Li. “Multiatom and resonant interaction scheme for quantum state transfer and logical gates between two remote cavities via an optical fiber.” Physical Review A 75.1 (2007): 012324.
- [4] Westermann, Sebastian, et al. “Dynamics of resonant energy transfer in a cold Rydberg gas.” The European Physical Journal D-Atomic, Molecular, Optical and Plasma Physics 40.1 (2006): 37-43.
- [5] Anderson, W. R., J. R. Veale, and T. F. Gallagher. “Resonant dipole-dipole energy transfer in a nearly frozen rydberg gas.” Physical review letters 80.2 (1998): 249.
- [6] Vogt, Thibault, et al. “Dipole blockade at Frster resonances in high resolution laser excitation of Rydberg states of cesium atoms.” Physical review letters 97.8 (2006): 083003.
- [7] Gurian, J. H., et al. “Observation of a resonant four-body interaction in cold cesium Rydberg atoms.” Physical review letters 108.2 (2012): 023005.
- [8] Jaksch, D., et al. “Fast quantum gates for neutral atoms.” Physical Review Letters 85.10 (2000): 2208.
- [9] Lukin, M. D., et al. “Dipole blockade and quantum information processing in mesoscopic atomic ensembles.” Physical Review Letters 87.3 (2001): 037901.
- [10] Ricci, L., et al. “A compact grating-stabilized diode laser system for atomic physics.” Optics Communications 117.5 (1995): 541-549.
- [11] Coldren, Larry A., Scott W. Corzine, and Milan L. Mashanovitch. *Diode lasers and photonic integrated circuits*. Vol. 218. John Wiley & Sons, 2012.

[12] Harvey, K. C., and C. J. Myatt. "External-cavity diode laser using a grazing-incidence diffraction grating." *Optics Letters* 16.12 (1991): 910-912.

[13] Riedle, Eberhard, et al. "Stabilization and precise calibration of a continuous?wave difference frequency spectrometer by use of a simple transfer cavity." *Review of scientific instruments* 65.1 (1994): 42-48.

[14] "Microchannel Plates."

<http://www.mi.infn.it/~sleoni/TEACHING/Nuc-Phys-Det/PDF/papers/MCP.pdf>.

[15] Miroshnychenko, Yevhen, et al. "Coherent excitation of a single atom to a Rydberg state." *Physical Review A* 82.1 (2010): 013405.

[16] Zhao, W. Z., et al. "A computer-based digital feedback control of frequency drift of multiple lasers." *Review of scientific instruments* 69.11 (1998): 3737-3740.

[17] Donley, E. A., et al. "Double-pass acousto-optic modulator system." *Review of Scientific Instruments* 76.6 (2005): 063112.

[18] "Moglabs wavemeter."

[http://www.moglabs.com/uploads/2/4/2/1/24212474/moglabs\\_wavemeter\\_manual\\_rev097.pdf](http://www.moglabs.com/uploads/2/4/2/1/24212474/moglabs_wavemeter_manual_rev097.pdf).

[19] "Saturated Absorption Spectroscopy." PHY4803L- Advanced Physics Laboratory. University of Florida Department of Physics (2014).

[20] Brandenberger, John. "Doppler-Free Spectroscopy." MIT Department of Physics (2012).

[21] Paschotta, Rüdiger. Tunable lasers. [https://www.rp-photonics.com/tunable\\_lasers.html](https://www.rp-photonics.com/tunable_lasers.html).